Trapping the transition state of an ATP-binding cassette transporter: Evidence for a concerted mechanism of maltose transport

Jue Chen*, Susan Sharma†, Florante A. Quiocho*‡, and Amy L. Davidson†§

*Howard Hughes Medical Institute, and Departments of †Molecular Virology and Microbiology and ‡Biochemistry and Molecular Biology, Baylor College of Medicine, One Baylor Plaza, Houston, TX 77030

High-affinity uptake into bacterial cells is mediated by a large class of periplasmic binding protein-dependent transport systems, members of the ATP-binding cassette superfamily. In the maltose transport system of *Escherichia coli*, the periplasmic maltose-binding protein binds its substrate maltose with high affinity and, in addition, stimulates the ATPase activity of the membrane-associated transporter when maltose is present. Vanadate inhibits maltose transport by trapping ADP in one of the two nucleotide-binding sites of the membrane transporter immediately after ATP hydrolysis, consistent with its ability to mimic the transition state of the γ-phosphate of ATP during hydrolysis. Here we report that the maltose-binding protein becomes tightly associated with the membrane transporter in the presence of vanadate and simultaneously loses its high affinity for maltose. These results suggest a general model explaining how ATP hydrolysis is coupled to substrate transport in which a binding protein stimulates the ATPase activity of its cognate transporter by stabilizing the transition state.

ATP binding cassette (ABC) transporters are found in each of the phylogenetic kingdoms (1). ABC proteins have been identified that function in an increasing variety of uptake and efflux functions, including nutrient transport, protein and peptide transport, polysaccharide transport, and ion transport. Some ABC transporters function as multidrug efflux pumps in both prokaryotes and eukaryotes, and overexpression of the mammalian multidrug resistance protein MDR is sometimes responsible for multidrug resistance after chemotherapy in human cancer (2). Several human diseases have been traced to ABC proteins, including cystic fibrosis, hyperinsulinemia, and macular dystrophy (1, 3–5), making it important to understand their mechanism of action. The maltose transport system, one of at least 50 such systems in *Escherichia coli* (6), is well characterized both genetically and biochemically and provides an excellent model system for study of the ABC family (7). It consists of a periplasmic maltose-binding protein (MBP) and a multisubunit ABC transporter (MalFGK$_2$) containing two membrane integral subunits (MalF and MalG) and two copies of a peripheral subunit (MalK) that hydrolyzes ATP (7, 8). MBP functions as the primary receptor for maltose, undergoing a conformational change to encapsulate the sugar and generate a high-affinity protein–ligand complex (9, 10). Maltose-loaded MBP then interacts with MalFGK$_2$ to stimulate ATP hydrolysis by MalK (11) and initiate the transport process. The mechanism by which MBP stimulates ATP hydrolysis is unknown, nor is it known how maltose is transferred from the high-affinity site in MBP to MalFGK$_2$.

We believe that many of these details can be elucidated by stabilizing and characterizing intermediates in the transport pathway. Vanadate, an analogue of inorganic phosphate, acts as a potent inhibitor of many ATPases, presumably because it can mimic the transition state for the γ-phosphate of ATP during hydrolysis and stabilize the transition state conformation (12, 13). In the structure of myosin in complex with vanadate, ADP

is stably trapped in the catalytic site, with vanadate occupying the position of the γ-phosphate, in the transition state conformation (14). Vanadate has been shown to inhibit several of the ABC transporters, including the maltose transport system, by stably trapping ADP in the active site (15–18). Potent inhibition by vanadate, in combination with observed trapping of ADP and a requirement for ATP hydrolysis in the formation of the vanadate-inhibited species, is taken as evidence that vanadate is acting as a transition state analogue in the case of the ABC transporters (17, 19). In the case of the maltose transport system, the requirement for ATP hydrolysis was clearly demonstrated by the requirement for Mg, ATP, and MBP in the formation of the vanadate-inhibited species, and ADP would not substitute for ATP (18). In this report we further characterize the vanadate-inhibited maltose transporter and find that MBP, but not maltose, is tightly bound to MalFGK$_2$. These results offer considerable insight into what happens during the transport cycle of an ABC transporter.

Materials and Methods

Purification and Reconstitution of the Maltose Transport Complex.
MalF, MalG, and a derivative of MalK containing an N-terminal polyhistidine tag were overexpressed in *E. coli* as described (18, 20). These three proteins form a tetramer (MalFGK$_2$) in the membrane that remains intact during solubilization and purification. Isolated membrane fractions (3 mg protein/ml) were treated with 1% *n*-dodecyl-β-D-maltoside in buffer containing 20 mM Hepes (pH 8), 5 mM MgCl$_2$, and 10% glycerol to solubilize MalFGK$_2$. MalFGK$_2$ was bound to a cobalt affinity resin (CLONTECH) via the polyhistidine tag on the MalK subunit and eluted with imidazole as described (18). Preparations were greater than 90% pure, as judged by SDS/PAGE (data not shown). For reconstitution, purified complexes were dialyzed to remove imidazole and mixed with sonicated L-α-phosphatidylcholine (Sigma; P-5638) at a lipid-to-protein ratio (mg/mg) of 50:1 in the presence of 1% octyl β-D-glucopyranoside. Proteoliposomes were formed after a 25-fold dilution into 20 mM Hepes (pH 8) as described (8) and either used fresh or stored frozen at −70°C in aliquots until use. MBP was purified by affinity chromatography on amylose resin (21).

Assay of Maltose Transport and ATP Hydrolysis Activities. The ATPase activity of proteoliposomes containing purified, reconstituted MalFGK$_2$ was assayed as described with the use of

BIOCHEMISTRY

1 mM [γ-^{32}P]ATP and 5 μM MBP (18). Assays typically contained 0.04 μM MalFGK$_2$ and were initiated by addition of the proteoliposomes to other assay components pre-equilibrated at 37°C. The high Mg concentration used in this assay permeabilizes the proteoliposomes, allowing for assay of the MBP-stimulated ATPase activity of all transport complexes (22).

Maltose transport activity was assayed by the addition of proteoliposomes (final concentration 0.1 μM) to a mixture of 1 μM MBP and 10 μM [^{14}C]maltose and monitoring of the uptake into the vesicles at 23°C (23). For this assay, proteoliposomes were frozen and thawed twice in the presence of 5 mM MgATP to trap nucleotide inside, then passed 10 times through a 200-μm filter with the use of an extrusion device (Lipex Biomembranes) to regenerate unilamellar vesicles (24). To measure initial rates of transport with the limited amount of ATP that can be trapped inside the vesicles, only 1 μM MBP was used in the assay. Because the transporters can be reconstituted into lipid vesicles in two different orientations, only a fraction of the transporters are sampled by this uptake assay.

Estimation of Molar Concentrations of Nucleotide and Protein in the Vanadate-Trapped Species. Sodium orthovanadate, prepared according to the method of Goodno (12), was boiled immediately before use. Incubation of MalFGK$_2$ with vanadate is described in the legends to Figs. 1 and 2. The molar ratio of nucleotide to protein in the vanadate-trapped complex was determined essentially as described (18). Briefly, [α-^{32}P]ATP was incubated with vanadate and protein, and bound nucleotide was separated from unbound nucleotide by gel filtration (Amersham Pharmacia; HiTrap, desalting) and ion exchange chromatography (Amersham Pharmacia; HiTrap, Q Sepharose). The molar ratio of MBP to MalFGK$_2$ in the vanadate-trapped MBP-MalFGK$_2$ complex was estimated from the intensity of the bands on Coomassie-stained SDS-polyacrylamide gels (11%). For comparative purposes, equal molar concentrations of MBP, MalFGK$_2$, and MBP-MalFGK$_2$ were loaded on gels and quantitated with a Nucleovision imaging system (data not shown). The concentration of each sample was assessed beforehand by amino acid analysis (Protein Chemistry Core Facility, Baylor College of Medicine).

Results

Previously we showed that vanadate inhibits the ATPase activity of MalFGK$_2$ by stably trapping ADP in the catalytic site after ATP hydrolysis and phosphate release (18). We hypothesize that vanadate has trapped MalFGK$_2$ in the transition state because catalysis is required to form the vanadate-inhibited species (18). Here we determined whether any other components of the transport system, including MBP or maltose, are tightly bound to the vanadate-inhibited MalFGK$_2$ species. The vanadate-inhibited transporter was formed by incubating proteoliposome vesicles containing purified MalFGK$_2$ with a molar excess of maltose-MBP, MgATP, and vanadate. The extent of inhibition by vanadate was assessed by assaying both maltose transport and ATPase activities. In the absence of vanadate, maltose was transported at a rate of 1.2 nmol/min/mg protein, and ATP was hydrolyzed at a rate of 4 μmol/min/mg (Fig. 1 A and B). The large difference in rates likely reflects both differences between the two assay systems (see *Materials and Methods*) and the variable stoichiometry of the coupling reaction reported previously *in vitro* (23, 25). Ninety percent of both the maltose transport and ATPase activities was stably inhibited after free vanadate was removed (Fig. 1 A and B). After centrifugation to separate soluble MBP from proteoliposomes, we found that MBP remained associated with the proteoliposome pellet after treatment with MgATP and vanadate, but that none was associated if either MgATP or vanadate was omitted from the
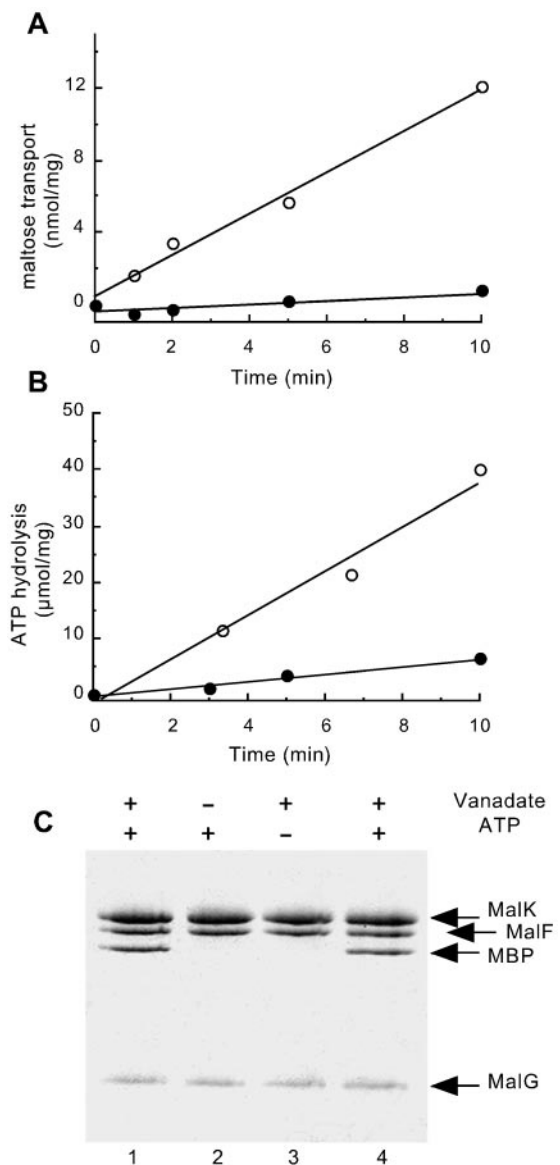
Fig. 1. Analysis of vanadate-treated proteoliposomes. Purified MalFGK$_2$ (2.5 μM) (18), reconstituted in proteoliposomes, was incubated with 5 μM purified MBP (21), 14 mM MgCl$_2$, 4 mM ATP, and 0.1 mM maltose for 20 min at 37°C in the presence (●) or absence (○) of 0.5 mM vanadate. Proteoliposomes were then diluted 20-fold in 20 mM Hepes (pH 8)/0.1 mM EDTA, collected by centrifugation, and suspended in Hepes/EDTA buffer. (*A*) [^{14}C]Maltose uptake into proteoliposomes (see *Materials and Methods*). (*B*) ATPase activity (see *Materials and Methods*) is measured on the same freeze/thawed proteoliposome preparation that was used for the transport measurements. (Proteoliposomes were washed by centrifugation to remove excess unlabeled ATP before assay.) (*C*) The protein content of proteoliposome pellets is visualized by Coomassie staining after SDS/PAGE. Lanes 1–3: Proteoliposomes incubated in the presence or absence of vanadate and ATP as indicated. Lane 4: Sample treated as in lane 1, but with 20 μM MBP.

incubation (Fig. 1C). The conditions promoting an interaction between MBP and proteoliposomes are identical to the conditions promoting formation of the vanadate-inhibited MalFGK$_2$ transporter (18), suggesting that MBP binds tightly to the vanadate-inhibited species. Increasing the amount of MBP used did not increase the recovery of MBP in the pellet (Fig. 1C, lane 4), reflecting saturation of binding sites in the proteoliposomes.

Stronger evidence for a high-affinity protein–protein interaction between MBP and the vanadate-inhibited transporter was
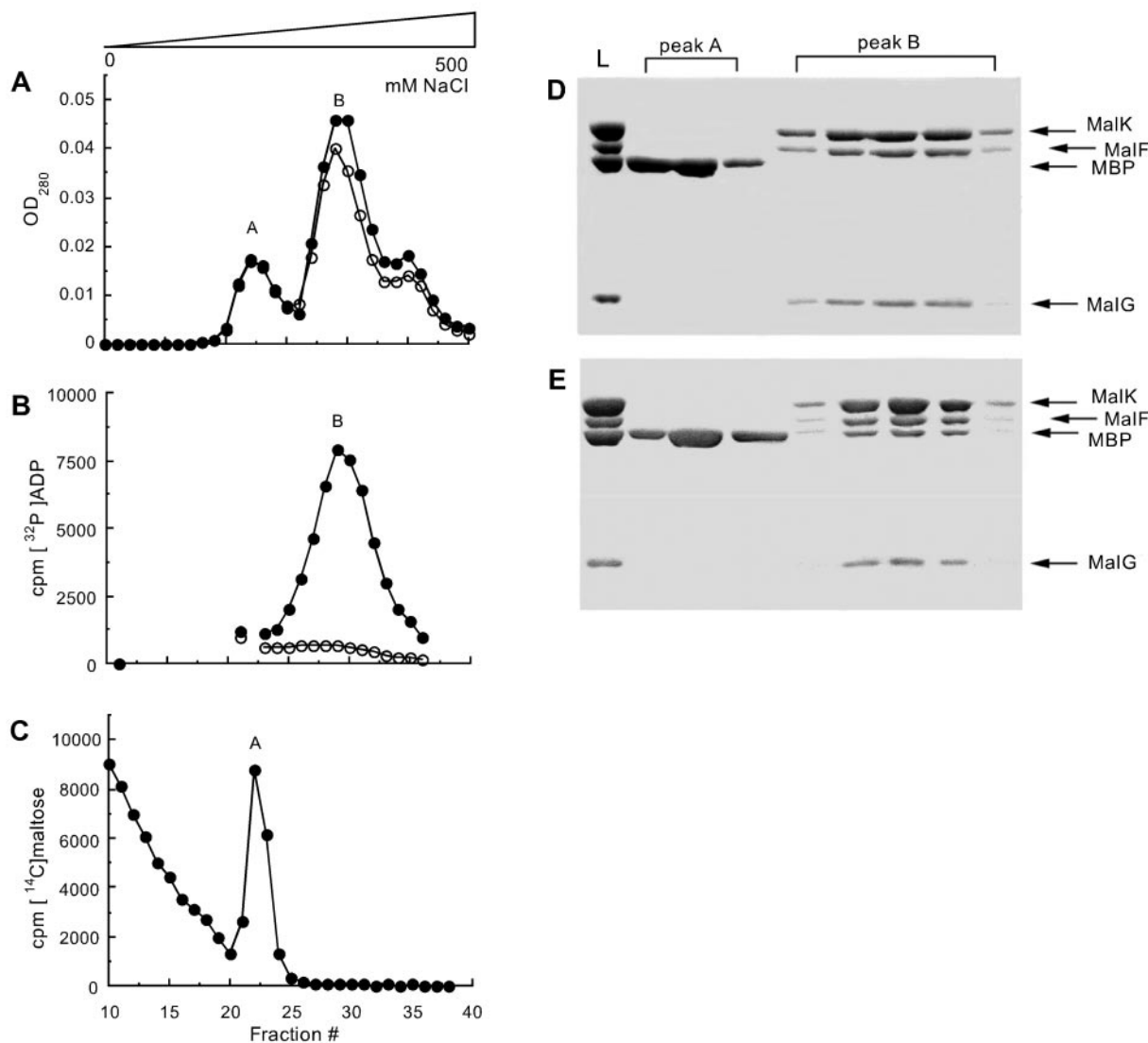
Fig. 2. Formation of a stable complex between MBP and MalFGK$_2$ in detergent solution. MalFGK$_2$ (2.5 μM) in 20 mM Hepes (pH 8), 10% glycerol, and 0.01% n-dodecyl-β-D-maltoside (exhibiting 0.2 μmol/min/mg of ATPase activity) was incubated with 5 μM MBP, 4 mM MgCl$_2$, and 4 mM ATP for 20 min at 37°C in the presence (●) or absence (○) of 0.5 mM vanadate, then loaded onto a HiTrap Q Sepharose column (Amersham Pharmacia) and eluted with a gradient of NaCl. (A) OD$_{280}$ of fractions eluting during the gradient. (B) Radioactive elution profile of a sample incubated in the presence of 1 mM MgCl$_2$ and 0.8 mM [α-^{32}P]ATP in place of unlabeled ATP. The sample is desalted before ion exchange. (C) Radioactive elution profile of a sample incubated in the presence of 0.5 mM vanadate and 10 μM [^{14}C]maltose in place of unlabeled maltose. The sample is desalted before ion exchange. (D) Protein composition of fractions from a sample incubated in the absence of vanadate, visualized by Coomassie staining after SDS/PAGE. L, loaded sample. (E) Protein composition of fractions from a sample incubated in the presence of vanadate.

obtained with MBP and MalFGK$_2$ in detergent solution, eliminating the presence of lipid vesicles. The actual percentage inhibition of ATPase activity by vanadate treatment could not be accurately assessed in detergent because of the limited ability of MBP to stimulate the ATPase activity of detergent solubilized MalFGK$_2$. In the absence of vanadate, MBP and MalFGK$_2$ could be separated by ion exchange chromatography in detergent solution (Fig. 2 *A* and *D*). After incubation with vanadate and MgATP, MBP coeluted with MalFGK$_2$, demonstrating a high-affinity interaction between MBP and MalFGK$_2$ (Fig. 2 *A* and *E*). The stoichiometry of this complex, as judged from the intensity of the bands on SDS/PAGE (see *Materials and Methods*) was approximately one MBP per transporter. As shown previously in experiments with proteoliposomes (18), radioactivity from [α-^{32}P]ATP coeluted with MalFGK$_2$ only in the

presence of vanadate (Fig. 2*B*), indicating the trapping of ADP by vanadate. We estimate from this experiment that 0.9 mol of nucleotide was bound per mole of protein (assuming a molecular weight of 210,000 for the MBP-MalFGK$_2$ complex). The purified MBP-MalFGK$_2$ complex remains intact even after subsequent gel filtration chromatography (Fig. 3), further demonstrating the stability of this complex in detergent solution.

To determine whether maltose is also present in the vanadate-inhibited complex, MBP and detergent-soluble MalFGK$_2$ were incubated with [^{14}C]maltose, vanadate, and MgATP; desalted; and then separated by ion exchange chromatography (Fig. 2*C*). In contrast to ADP (Fig. 2*B*), [^{14}C]maltose coeluted with free MBP but not with MBP-MalFGK$_2$. Essentially the same result was obtained when the experiment was performed with proteoliposomes (data not shown), suggesting that the absence of

A

B
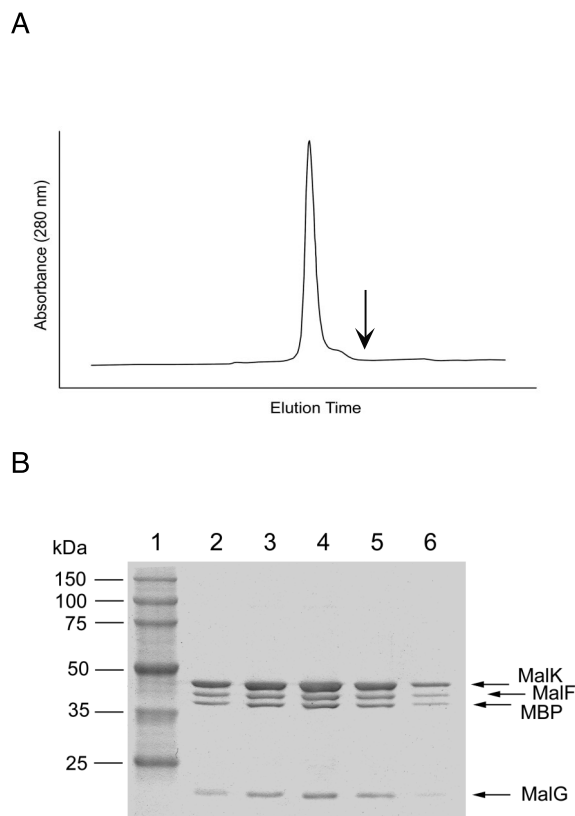
Fig. 3. Gel filtration of the MBP-MalFGK$_2$ complex. After ion-exchange chromatography, fractions containing peak B (Fig. 2*E*) were pooled, dialyzed against 20 mM Hepes (pH 8.0) and 0.01% *n*-dodecyl-β-D-maltoside, and stored for 30 days at −70°C. This purified material was thawed and subjected to gel filtration chromatography on a Superose 6 column (Amersham Pharmacia). (*A*) Elution profile of the gel filtration column. (*B*) Protein composition of peak fractions from *A*, visualized by SDS/PAGE and Coomassie staining of 8–25% gradient gels. Lane 1, Molecular weight markers. Lanes 2–6, Contiguous fractions across the emission peak. The expected position of elution of free MBP is indicated by the arrow.

maltose from the trapped MBP-MalFGK$_2$ complex is not solely an artifact of the use of a detergent-solubilized system. MBP binds maltose with a dissociation constant of 1 μM and exhibits a retention effect (26) that accounts for the slow release of maltose from MBP during ion exchange chromatography (Fig. 2*C*). The absence of maltose from the trapped complex indicates that maltose has been released from MBP by the time that vanadate acts to stabilize this transient intermediate.

Discussion

We have shown that MBP is tightly bound to the vanadate-inhibited MalFGK$_2$ species and that maltose is absent from this inhibited complex. These results fundamentally alter our view of the transport process. We had shown previously that MBP stimulates the ATPase activity of MalFGK$_2$ (11) and that MBP is required to form the vanadate-inhibited MalFGK$_2$ species (18). The fact that MBP is tightly bound to the vanadate-inhibited species suggests that the interaction of MBP with MalFGK$_2$ stimulates the ATPase activity of MalFGK$_2$ by stabilizing the transition state conformation of the transporter, thereby lowering the activation energy for hydrolysis. The absence of tightly bound maltose from the vanadate-stabilized MBP-MalFGK$_2$ complex is remarkable, given how difficult it is
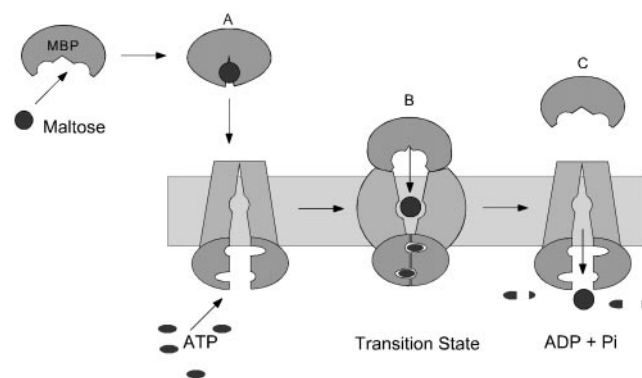
Fig. 4. A model for maltose transport. (*A*) MBP binds maltose and undergoes a conformational change from an open to a closed conformation, generating a high-affinity sugar-binding site. In the closed conformation, MBP binds MalFGK$_2$ to initiate transport and hydrolysis. (*B*) In the transition state, MBP and MalFGK$_2$ become tightly bound to each other, and both proteins have opened, exposing internal binding sites to each other. Opening of MBP in the transition state weakens the interaction between MBP and maltose, facilitating the transfer of sugar to the low-affinity binding site in MalFGK$_2$. (*C*) Maltose is transported and MBP is released after the re-exposure of the internal binding site to the cytoplasm. The MalK subunits are modeled after the Rad50 catalytic domain structure (33). This ABC protein undergoes an ATP-induced dimerization and activation step that completes both nucleotide-binding sites with residues donated from the opposing subunit. By analogy, MBP may stimulate the ATPase activity of MalK by bringing the two subunits into close proximity in the transition state.

to obtain preparations of maltose-free MBP (26), and suggests that transport has occurred before the formation of the vanadate-inhibited complex. We propose that the tight binding interactions between MBP and MalFGK$_2$ that stabilize the transition state may also abrogate high-affinity sugar binding to MBP, facilitating the transfer of maltose to MalFGK$_2$, which contains a low-affinity maltose-binding site (27). Maltose binds with high affinity to MBP in a cleft between two domains connected by a flexible hinge, where it contacts both domains (9). This closed conformation of MBP is in equilibrium with a more open conformation where maltose contacts only one domain and dissociates more readily (28). Thus it is probable that MBP is in a conformation resembling the open conformation when it is tightly bound to MalFGK$_2$, thereby reducing its affinity for maltose.

The main points of our findings are summarized in a model for maltose transport that is presented in Fig. 4. In contrast to some earlier models in which MalK homologues span the membrane (29), we depict the MalK subunits as being only peripherally associated with the MalF and MalG proteins, in accordance with crystal structures indicating that they are globular in nature (30–33). MBP in the closed-liganded conformation initiates transport by interacting with MalFGK$_2$. In keeping with the mobile barrier model of Mitchell (34), we have the sugar-binding site in MalFGK$_2$ initially accessible only from the cytoplasm. In the transition state for ATP hydrolysis, when MBP is tightly bound and displays a low affinity for maltose, the binding site in MalFGK$_2$ is oriented toward the periplasm to capture maltose as it is released from MBP. After receiving the sugar, the binding site reorients to the cytoplasm so that maltose is released inside the cell. In essence, essentially all of the key reactions required for transport may occur simultaneously through concerted conformational changes in the MBP-MalFGK$_2$ transient that are directly coupled to ATP hydrolysis in the transition state. Before this time, the transport process had been viewed as a sequential series of events (7, 29). The model in Fig. 4 predicts

that maltose might be trapped within a pocket formed by MBP and MalFGK$_2$ in the transition state. If the binding site in MalFGK$_2$ faces the periplasm only in the transition state, the sugar may be released to the cytoplasm before vanadate trapping, accounting for the absence of maltose in the vanadate-inhibited species. Alternatively, an open channel may span the membrane in the transition state with MBP blocking exit to the periplasm, so that maltose is released directly into the cytoplasm. The recent structure of the Rad50 catalytic domain, an ABC protein involved in DNA double-strand break repair (33), may offer further insight into the mechanism of activation of the ATPase activity of MalFGK$_2$ by MBP. ATP promotes dimerization of two Rad50 catalytic domains in a head-to-tail conformation, thereby completing both nucleotide binding sites with residues donated from the opposing subunit. It is possible that MBP regulates the ATPase activity of MalFGK$_2$ by promoting cycles of association and dissociation of the two MalK subunits in the transport complex.

Although the periplasmic binding protein-dependent transport systems are the only members of the ABC family that use accessory proteins to bind substrate, some features of this proposed mechanism may be conserved. The multiple-drug-resistance pumps MDR and LmrA appear to have both low- and high-affinity drug-binding sites, and formation of the vanadate-inhibited species is associated with the loss of high-affinity drug binding (35, 36). These sites may be analogous to the high- and low-affinity binding sites in MBP and MalFGK$_2$, respectively. Coupling of ATP hydrolysis to conformational changes that eliminate high-affinity binding in the transition state will facilitate the transfer of substrate to the low-affinity site and ultimately across the membrane. A second feature that is conserved in ABC transporters is the cooperativity of the two nucleotide-binding sites (20, 37–39). In both MDR and MalFGK$_2$ transporters, trapping of ADP by vanadate in one nucleotide-binding site inhibits the ATPase activity of both sites (17, 18).

The high affinity that MBP displays for MalFGK$_2$ in the presence of vanadate is reminiscent of the interaction between the Ras-GTPase and its regulatory protein, GTPase-activating protein (GAP), and between the two components of nitrogenase (40, 41). The basal rate of GTP hydrolysis by Ras is very slow, and GAP stimulates the activity by several orders of magnitude (42). Aluminum fluoride, like vanadate, stabilizes a transition state complex of GDP-Ras and GAP. Structural analysis reveals that GAP stimulates the GTPase activity of Ras by contributing an additional catalytic residue to the active site to stabilize the transition state (43). RGS proteins (regulators of G-protein signaling) function as GAPs by repositioning catalytic residues already present in the active site of their G-protein partners (44). In the nitrogenase reaction, ATP hydrolysis is coupled to the transfer of electrons between two proteins, neither of which hydrolyzes ATP in the absence of the other. Aluminum fluoride traps a transition state complex of the two proteins in which the two metal clusters involved in the electron transfer reaction (one in each protein) are positioned directly across from each other, facilitating transfer (41). We have predicted that, in the transition state complex of MBP and MalFGK$_2$, the two maltose-binding sites are similarly juxtaposed to facilitate the transfer of sugar from one protein to the next (Fig. 4). The maltose system, however, has greater complexity than nitrogenase because the ATPase-activating protein MBP and the MalK ATPase are located on opposite sides of the cytoplasmic membrane, and conformational signaling between these two proteins must occur via the transmembrane proteins MalF and MalG.

Our study uses a transition state analogue to stabilize transient interactions between components of a membrane transport system. Binding-protein-dependent transporters are unlikely to be the only transporters that employ a G-protein-like regulatory mechanism. For example, in protein translocation systems, where a soluble ATPase component is often regulated by its interaction with a membrane-embedded transporter (45, 46), a transition state analogue such as vanadate may help to characterize the interaction. In Gram-negative bacteria, ABC proteins mediating export from Gram-negative bacteria form transient complexes with inner and outer membrane proteins that might also be stabilized by vanadate (47). Our results offer the possibility of isolating and carrying out structural studies on transport intermediates that will elucidate fundamental mechanisms of transport and coupling to ATP hydrolysis.

1. Holland, I. B. & Blight, M. A. (1999) *J. Mol. Biol.* **293,** 381–399.
2. Chen, C.-J., Chin, J. E., Ueda, K., Clark, D. P., Pastan, I., Gottesman, M. M. & Roninson, I. G. (1986) *Cell* **47,** 381–389.
3. Rich, D. P., Anderson, M. P., Gregory, R. J., Cheng, S. H., Paul, S., Jefferson, D. M., McCann, J. D., Klinger, K. W., Smith, A. E. & Welsh, M. J. (1990) *Nature (London)* **347,** 358–363.
4. Thomas, P. M., Cote, G. J., Wohllk, N., Haddad, B., Mathew, P. M., Rabl, W., Aguilar-Bryan, L., Gagel, R. F. & Bryan, J. (1995) *Science* **268,** 426–429.
5. Allikmets, R., Singh, N., Sun, H., Shroyer, N. F., Hutchinson, A., Chidambaram, A., Gerrard, B., Baird, L., Stauffer, D., Peiffer, A., *et al.* (1997) *Nat. Genet*. **15,** 236–246.
6. Paulsen, I. T., Sliwinski, M. K. & Saier, M. H., Jr. (1998) *J. Mol. Biol.* **277,** 573–592.
7. Boos, W. & Lucht, J. M. (1996) in *Escherichia coli and Salmonella: Cellular and Molecular Biology*, eds. Neidhardt, F. C., Curtiss, R., III, Ingraham, J. L., Lin, E. C. C., Low, K. B., Magasanik, B., Reznikoff, W. S., Riley, M., Schaechter, M. & Umbarger, H. E. (Am. Soc. Microbiol., Washington, DC), Vol. 1, pp. 1175–1209.
8. Davidson, A. L. & Nikaido, H. (1991) *J. Biol. Chem.* **266,** 8946–8951.
9. Spurlino, J. C., Lu, G. Y. & Quiocho, F. A. (1991) *J. Biol. Chem.* **266,** 5202–5219.
10. Sharff, A. J., Rodseth, L. E., Spurlino, J. E. & Quiocho, F. A. (1992) *Biochemistry* **31,** 10657–10663.
11. Davidson, A. L., Shuman, H. A. & Nikaido, H. (1992) *Proc. Nat. Acad. Sci. USA* **89,** 2360–2364.
12. Goodno, C. C. (1982) *Methods Enzymol.* **85,** 116–123.
13. Shimizu, T. & Johnson, K. A. (1983) *J. Biol. Chem.* **258,** 13833–13840.
14. Smith, C. A. & Rayment, I. (1996) *Biochemistry* **35,** 5404–5417.
15. Taguchi, Y., Yoshida, A., Takada, Y., Komano, T. & Ueda, K. (1997) *FEBS Lett.* **401,** 11–14.
16. Szabo, K., Szakacs, G., Hegedus, T. & Sarkadi, B. (1999) *J. Biol. Chem.* **274,** 12209–12212.
17. Urbatsch, I. L., Sankaran, B., Weber, J. & Senior, A. E. (1995) *J. Biol. Chem.* **270,** 19383–19390.
18. Sharma, S. & Davidson, A. L. (2000) *J. Bacteriol.* **182,** 6570–6576.
19. Urbatsch, I. L., Sankaran, B., Bhagat, S. & Senior, A. E. (1995) *J. Biol. Chem.* **270,** 26956–26962.
20. Davidson, A. L. & Sharma, S. (1997) *J. Bacteriol.* **179,** 5458–5464.
21. Ferenci, T. & Klotz, U. (1978) *FEBS Lett.* **94,** 213–217.
22. Liu, C. E., Liu, P. Q. & Ames, G. F.-L. (1997) *J. Biol. Chem.* **272,** 21883–21891.
23. Davidson, A. L. & Nikaido, H. (1990) *J. Biol. Chem.* **265,** 4254–4260.
24. Liu, C. E. & Ames, G. F. (1997) *J. Biol. Chem.* **272,** 859–866.
25. Bishop, L., Agbayani, R., Jr., Ambudkar, S. V., Maloney, P. C. & Ames, G. F.-L. (1989) *Proc. Natl. Acad. Sci. USA* **86,** 6953–6957.
26. Silhavy, T. J., Szmelcman, S., Boos, W. & Schwartz, M. (1975) *Proc. Natl. Acad. Sci. USA* **72,** 2120–2124.
27. Treptow, N. A. & Shuman, H. A. (1985) *J. Bacteriol.* **163,** 654–660.
28. Ledvina, P. S., Tsai, A. L., Wang, Z., Koehl, E. & Quiocho, F. A. (1998) *Protein Sci.* **7,** 2550–2559.
29. Ames, G. F.-L., Mimura, C. S., Holbrook, S. R. & Shyamala, V. (1992) *Adv. Enzymol.* **65,** 1–47.
30. Hung, L. W., Wang, I. X., Nikaido, K., Liu, P. Q., Ames, G. F.-L. & Kim, S. H. (1998) *Nature (London)* **396,** 703–707.
31. Jones, P. M. & George, A. M. (1999) *FEMS Microbiol. Lett.* **179,** 187–202.

32. Diederichs, K., Diez, J., Greller, G., Muller, C., Breed, J., Schnell, C., Vonrhein, C., Boos, W. & Welte, W. (2000) *EMBO J.* **19,** 5951–5961.
33. Hopfner, K. P., Karcher, A., Shin, D. S., Craig, L., Arthur, L. M., Carney, J. P. & Tainer, J. A. (2000) *Cell* **101,** 789–800.
34. Mitchell, P. (1990) *Res. Microbiol.* **141,** 286–289.
35. Ramachandra, M., Ambudkar, S. V., Chen, D., Hrycyna, C. A., Dey, S., Gottesman, M. M. & Pastan, I. (1998) *Biochemistry* **37,** 5010–5019.
36. van Veen, H. W., Margolles, A., Muller, M., Higgins, C. F. & Konings, W. N. (2000) *EMBO J.* **19,** 2503–2514.
37. Berkower, C. & Michaelis, S. (1991) *EMBO J.* **10,** 3777–3785.
38. Loo, T. W. & Clarke, D. M. (1996) *J. Biol. Chem.* **270,** 21449–21452.
39. Davidson, A. L., Laghaeian, S. S. & Mannering, D. E. (1996) *J. Biol. Chem.* **271,** 4858–4863.
40. Mittal, R., Ahmadian, M. R., Goody, R. S. & Wittinghofer, A. (1996) *Science* **273,** 115–117.
41. Schindelin, H., Kisker, C., Schlessman, J. L., Howard, J. B. & Rees, D. C. (1997) *Nature (London)* **387,** 370–376.
42. Gideon, P., John, J., Frech, M., Lautwein, A., Clark, R., Scheffler, J. E. & Wittinghofer, A. (1992) *Mol. Cell Biol.* **12,** 2050–2056.
43. Scheffzek, K., Ahmadian, M. R., Kabsch, W., Wiesmuller, L., Lautwein, A., Schmitz, F. & Wittinghofer, A. (1997) *Science* **277,** 333–338.
44. Tesmer, J. J., Berman, D. M., Gilman, A. G. & Sprang, S. R. (1997) *Cell* **89,** 251–261.
45. Lill, R., Dowhan, W. & Wickner, W. (1990) *Cell* **60,** 271–280.
46. Minamino, T. & MacNab, R. M. (2000) *Mol. Microbiol.* **35,** 1052–1064.
47. Thanabalu, T., Koronakis, E., Hughes, C. & Koronakis, V. (1998) *EMBO J.* **17,** 6487–6496.